ADVANCED ELECTRONIC MATERIALS

Supporting Information

for *Adv. Electron. Mater.*, DOI: 10.1002/aelm.201500076

Unprecedentedly Wide Curie-Temperature Windows as Phase-Transition Design Platform for Tunable Magneto-Multifunctional Materials

Zhi-Yang Wei, En-Ke Liu, Yong Li, Gui-Zhou Xu, Xiao-Ming Zhang, Guo-Dong Liu, Xue-Kui Xi, Hong-Wei Zhang, Wen-Hong Wang,* Guang-Heng Wu, and Xi-Xiang Zhang*

Supporting Information

Unprecedentedly Wide Curie-Temperature Windows as Phase-Transition Design Platform for Tunable Magneto-Multifunctional Materials

Zhi-Yang Wei, En-Ke Liu, Yong Li, Gui-Zhou Xu, Xiao-Ming Zhang, Guo-Dong Liu, Xue-Kui Xi, Hong-Wei Zhang, Wen-Hong Wang,* Guang-Heng Wu, and Xi-Xiang Zhang*

Supporting Information

Unprecedentedly Wide Curie-Temperature Windows as Phase-Transition Design Platform for Tunable Magneto-Multifunctional Materials

Zhi-Yang Wei, En-Ke Liu, Yong Li, Gui-Zhou Xu, Xiao-Ming Zhang, Guo-Dong Liu, Xue-Kui Xi, Hong-Wei Zhang, Wen-Hong Wang,* Guang-Heng Wu, and Xi-Xiang Zhang*

X-ray diffraction (XRD) structural analysis. The powder X-ray diffraction measurements for y = 0.26, 0.36, 0.46 and 0.55 with various x in $Mn_{1-y}Fe_yNiGe_{1-x}Si_x$ system were performed on well-grinded powders. Upon the measurements, the scanning speed was set as 5 degree per minute. And the diffraction peaks from Cu $K\alpha_2$ radiation were carefully deducted. The data are shown in **Figure S1** below**.** Good diffraction quality was obtained for the samples with low-Si substitution to high-Si substitution for y = 0.26, 0.36, 0.46 and 0.55. The Ni_2In-type hexagonal parent structure and TiNiSi-type martensite structure are well identified in the diffraction patterns. The Miller indices $(hkl)_h$ and $(hkl)_o$ for parent and martensite structures were indexed. The results indicate that $Mn_{1-y}Fe_yNiGe_{1-x}Si_x$ alloys can well crystallize the desired phases for the strong degree of substitution with y = 0.26, 0.36, 0.46, 0.55 and $0 \leq x \leq 1$, which provides a critical fundament for the realization of our strongly-coupled magnetostructural transitions in an extremely wide temperature range.

After careful examinations, nevertheless, two extra small diffraction peaks were observed at around 37.6° and 45.4° in the XRD patterns of some alloy compositions (as pointed out with ♦ in **Figure S1**). In the present work, the samples were prepared by slow cooling with furnace after annealing, in order to get the equilibrium phase transitions without stress and disorders in samples. This impurity phase with very small amounts probably result from the precipitate during cooling process. Nevertheless, from the diffraction intensity the phase proportion of this impurity phase is rather low. One can see that, in general, this impurity phase imposes little influence on phase transitions and magnetic properties of the samples, which has also been evidenced by the regularity of Si-content dependence of both martensitic transition temperature and Curie temperature shown in the phase diagram and the M-T curves in **Figure 1**. Importantly, the highly tunable phase transitions and giant magnetocaloric effects were obtained in such an unprecedentedly wide temperature range. It is hopeful to avoid this small-amount impurity phase by quenching the samples after

annealing. Further optimizations and enhancements are expected in the important physical properties obtained in present work.

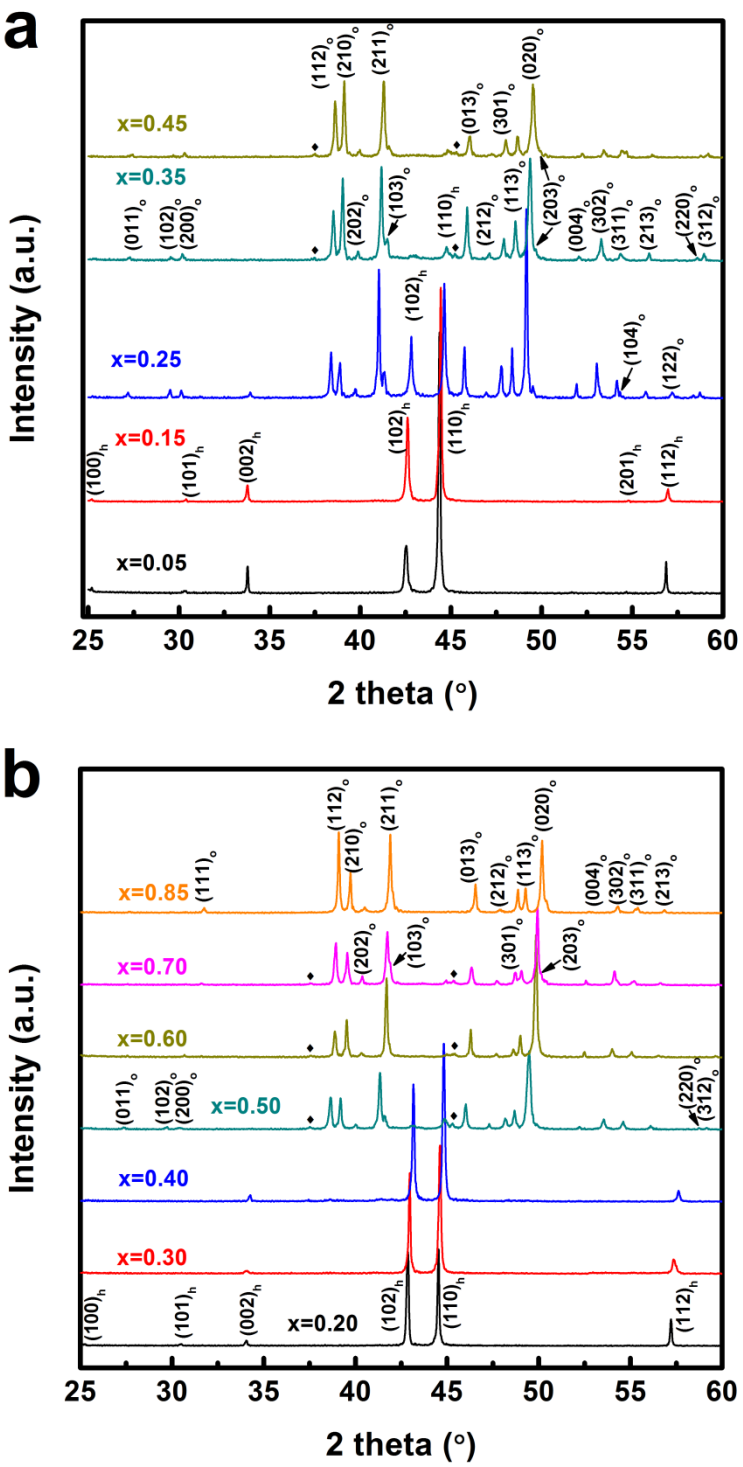

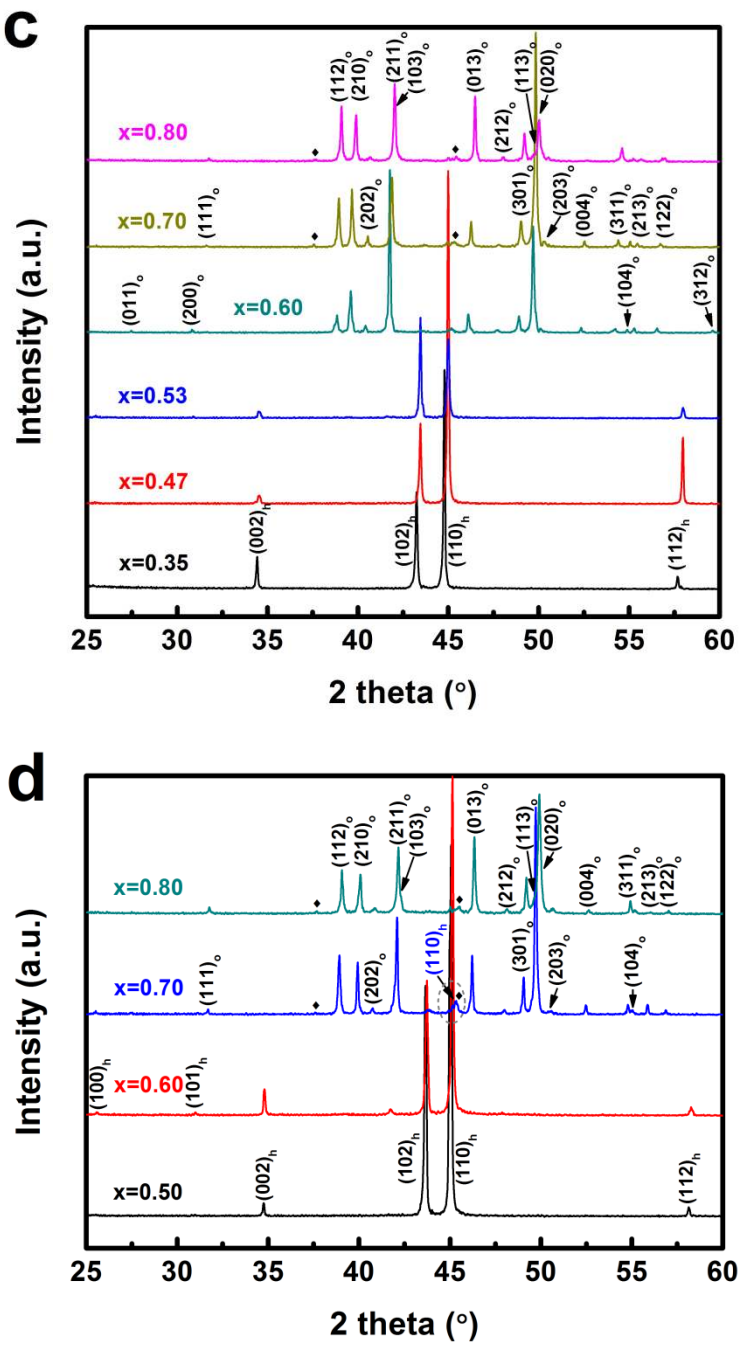

Figure S1. XRD patterns with various x for (a) $Mn_{0.74}Fe_{0.26}NiGe_{1-x}Si_x$, (b) $Mn_{0.64}Fe_{0.36}NiGe_{1-x}Si_x$, (c) $Mn_{0.54}Fe_{0.46}NiGe_{1-x}Si_x$, (d) $Mn_{0.45}Fe_{0.55}NiGe_{1-x}Si_x$.

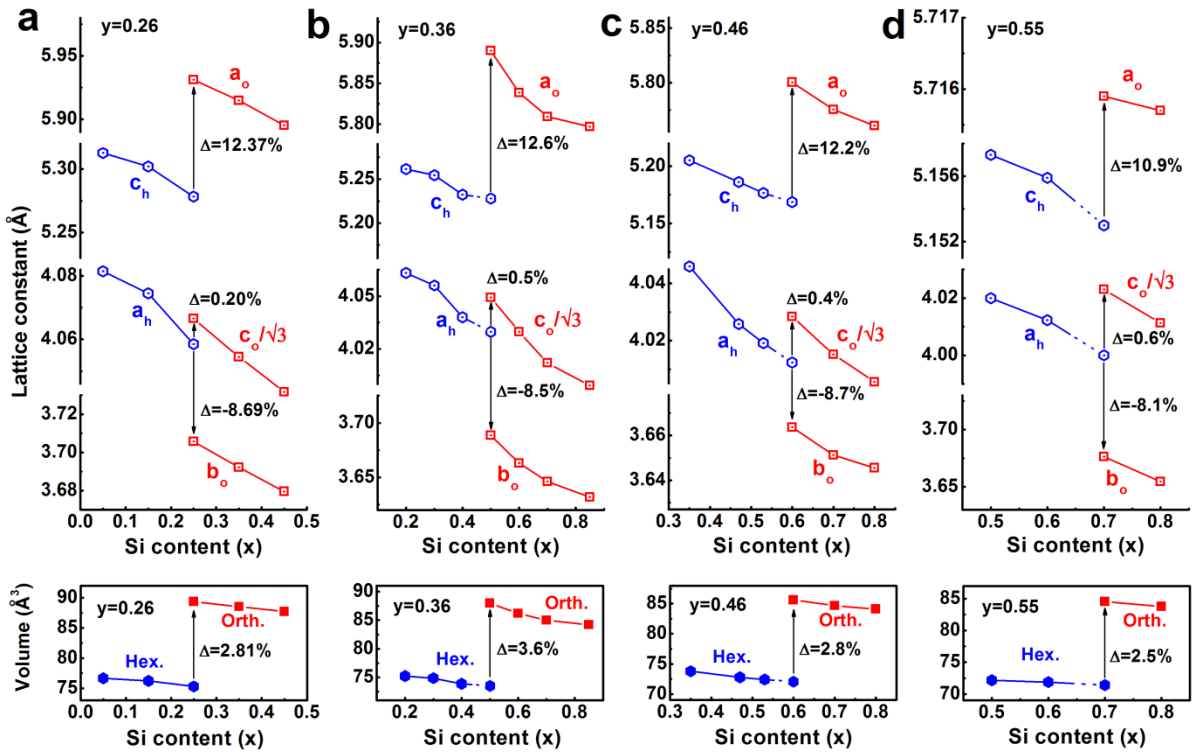

Figure S2. Si-content dependence of lattice constant and cell volume across the with martensitic transitions for (a) $Mn_{0.74}Fe_{0.26}NiGe_{1-x}Si_x$, (b) $Mn_{0.64}Fe_{0.36}NiGe_{1-x}Si_x$, (c) $Mn_{0.54}Fe_{0.46}NiGe_{1-x}Si_x$, (d) $Mn_{0.45}Fe_{0.55}NiGe_{1-x}Si_x$. The hexagonal parent and orthorhombic martensite phase are represented by subscript "h" and "o", respectively.

Lattice constant and cell volume across the martensitic transitions. The lattice constants of $Mn_{1-y}Fe_yNiGe_{1-x}Si_x$ alloys are deprived from fitting the XRD patterns in **Figure S1**, as depicted in **Figure S2**. The dash lines refer to the estimated data points. From the results, the lattice constants for both the parent and martensite phases decrease with increasing Si content for various y values, which can be ascribed to the smaller atom size of Si compared to Ge. The axes and volumes of the two structures are related as $a_o = c_h$, $b_o = a_h$, $c_o=\sqrt{3}a_h$, and $V_o = 2V_h$, and the distortion way of the lattice when the martensitic transition occurs are indicated by the arrows. Upon the martensitic transition, the extension along c_h reaches 12.37%, and the volume expansion is as large as 2.81% for $y = 0.26$. The detailed data of the lattice constants and volumes are shown in **Table S1**.

Table S1. Lattice constants and cell volumes of parent and martensite phases for $Mn_{1-y}Fe_yNiGe_{1-x}Si_x$ alloys.

	x	a_h [Å]	c_h [Å]	c_h/a_h	V_h [Å^3]	a_o [Å]	b_o [Å]	c_o [Å]	V_o [Å^3]	$\Delta V_{o\text{-}h}$** [%]
y=0.26	0.05	4.0814	5.3125	1.3016	76.6373	-	-	-	-	-
	0.15	4.0745	5.3020	1.3013	76.2288	-	-	-	-	-
	0.25	4.0585	5.2782	1.3005	75.2918	5.9311	3.7058	7.0434	77.4045	2.81
	0.35	-	-	-	-	5.9148	3.6923	7.0226	77.4045	-
	0.45	-	-	-	-	5.8952	3.6796	7.0034	76.6834	-
y=0.36	0.2	4.0633	5.2614	1.2949	75.2289	-	-	-	-	-
	0.3	4.0561	5.2544	1.2954	74.8637	-	-	-	-	-
	0.4	4.0380	5.2323	1.2958	73.8849	-	-	-	-	-
	0.5	4.030*	5.228*	1.297*	73.521*	5.8898	3.6886	7.0134	76.1850	3.6
	0.6	-	-	-	-	5.8386	3.6629	6.9798	74.6362	-
	0.7	-	-	-	-	5.8093	3.6462	6.9491	73.5958	-
	0.85	-	-	-	-	5.7971	3.6319	6.9269	72.9214	-
y=0.46	0.35	4.0459	5.2051	1.2865	73.7887	-	-	-	-	-
	0.47	4.0258	5.1860	1.2882	72.7893	-	-	-	-	-
	0.53	4.0191	5.1766	1.2880	72.4158	-	-	-	-	-
	0.6	4.012*	5.169*	1.288*	72.061*	5.8004	3.6636	6.9774	74.1361	2.8
	0.7	-	-	-	-	5.7755	3.6513	6.9546	73.3278	-
	0.8	-	-	-	-	5.7605	3.6455	6.9379	72.8469	-
y=0.55	0.5	4.02	5.1573	1.2829	72.1781	-	-	-	-	-
	0.6	4.0123	5.1559	1.2850	71.8823	-	-	-	-	-
	0.7	4.000*	5.153*	1.295*	71.402*	5.7159	3.6765	6.9680	73.2145	2.5
	0.8	-	-		-	5.7157	3.6546	6.9477	72.5638	-

*the estimated data.

**$\Delta V_{o\text{-}h} = V_o/V_h - 1$.

Magnetic measurements. The thermomagnetic curves (**Figure S3**) and isothermal magnetization curves (**Figure S4**) were measured for y = 0.26, 0.36, 0.46 and 0.55 with various x in $Mn_{1-y}Fe_yNiGe_{1-x}Si_x$ system. The thermomagnetic curves show that the magnetostructural transition temperature can be continuously tuned within a wide temperature range.

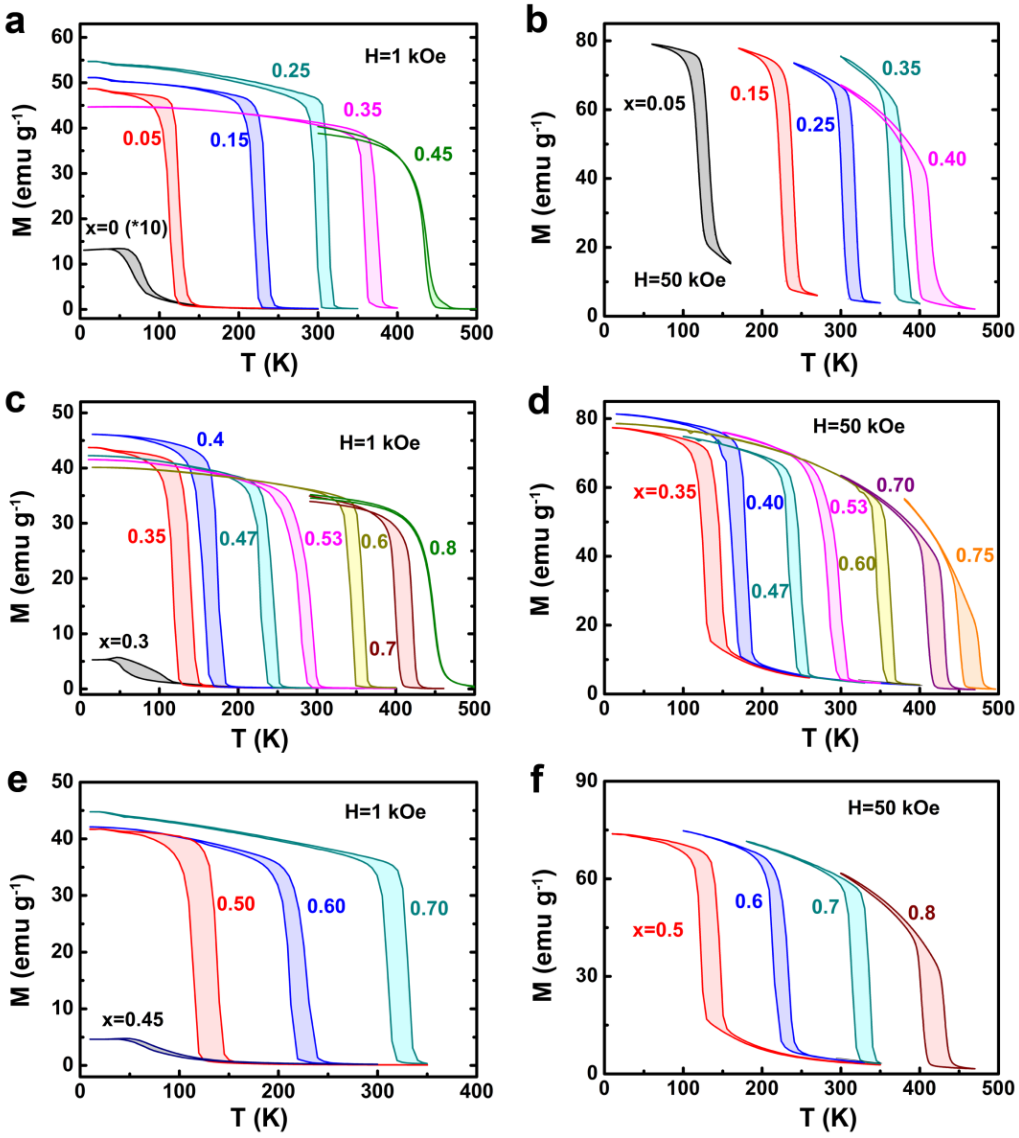

Figure S3. Thermomagnetic curves of $Mn_{1-y}Fe_yNiGe_{1-x}Si_x$ for (a) y = 0.26, (c) y = 0.46, and (e) y = 0.55, under magnetic field of 1 kOe, and for (b) y = 0.26, (d) y = 0.46, and (f) y = 0.55, under magnetic field of 50 kOe.

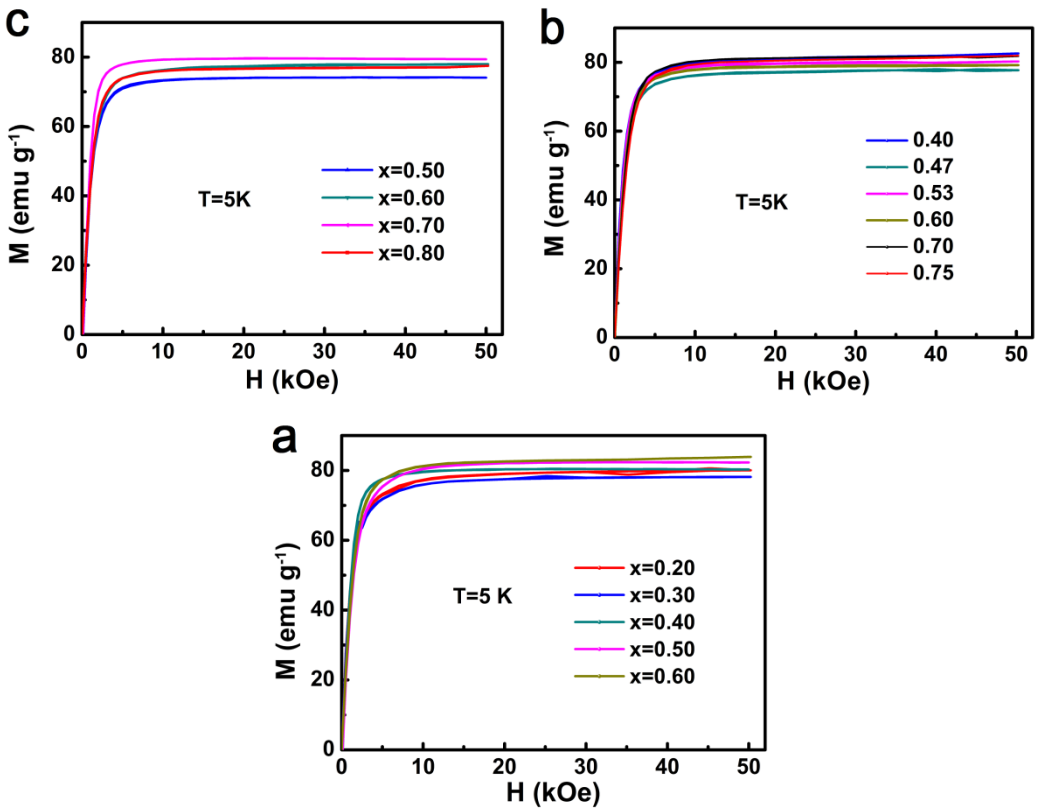

Figure S4. Isothermal magnetization curves of $Mn_{1-y}Fe_yNiGe_{1-x}Si_x$ for (a) y = 0.36, (b) y = 0.46, and (c) y = 0.55, at 5 K.

Thermal Measurements. Thermal analysis were performed on differential scanning calorimeter (DSC) for representative alloys with magnetostructural transition temperature from high (above room temperature, **Figure S5**) to low (**Figure S6**) temperatures. By adding an apparatus involving two permanent magnets to the high-temperature DSC, magnetic transition can be detected according to the thermal gravity (TG) change on the thermogravimetric analyzer. The big exothermic (endothermic) peak upon cooling (heating) on DSC curves indicates the (inverse) martensitic transitions. This first order phase transition shows apparent thermal hysteresis. In contrast, the rather small but observable peaks with no thermal hysteresis on DSC curves result from the magnetic transition at Curie temperature. The magnetic transitions (including magnetic ordering at Curie temperature and magnetostructural transitions) can be also revealed by the abrupt TG signal changes on corresponding TG curve. For a magnetostructural transition, the coupling of martensitic and magnetic transitions leads to a simultaneity between big exothermic peak on DSC curve and gravity change on TG curve upon cooling, as instance for the alloy (y = 0.36, x = 0.60) in **Figure S5**.

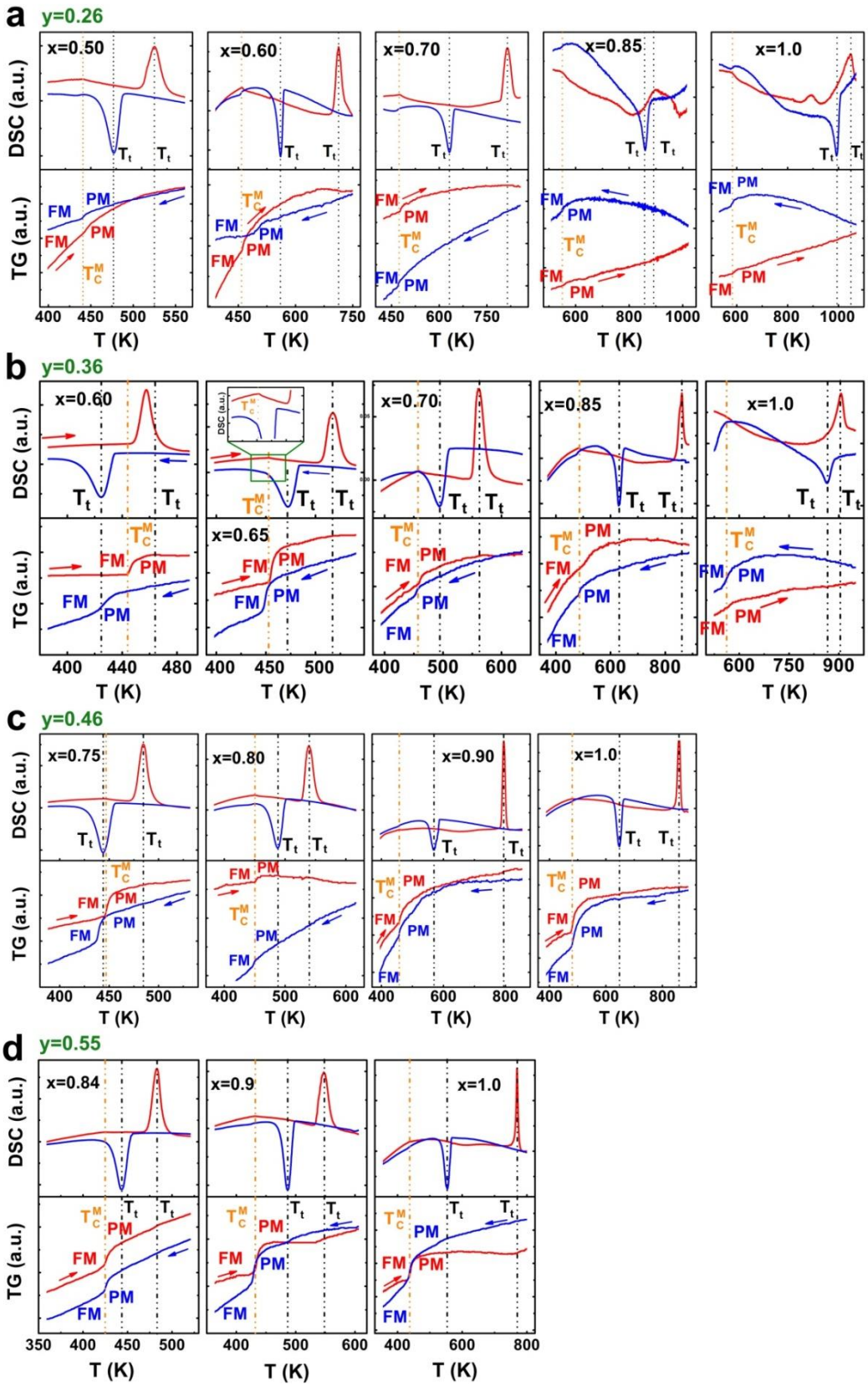

Figure S5. High-temperature DSC curves and relevant TG curves for $Mn_{1-y}Fe_yNiGe_{1-x}Si_x$ for (a) y = 0.26, (b) y = 0.36, (c) y = 0.46 and (d) y = 0.55. FM, PM, T_t and T_C^M refer to ferromagnetic, paramagnetic, martensitic transition temperature and Curie temperature of martensite, respectively. The red and blue lines correspond to heating and cooling process respectively.

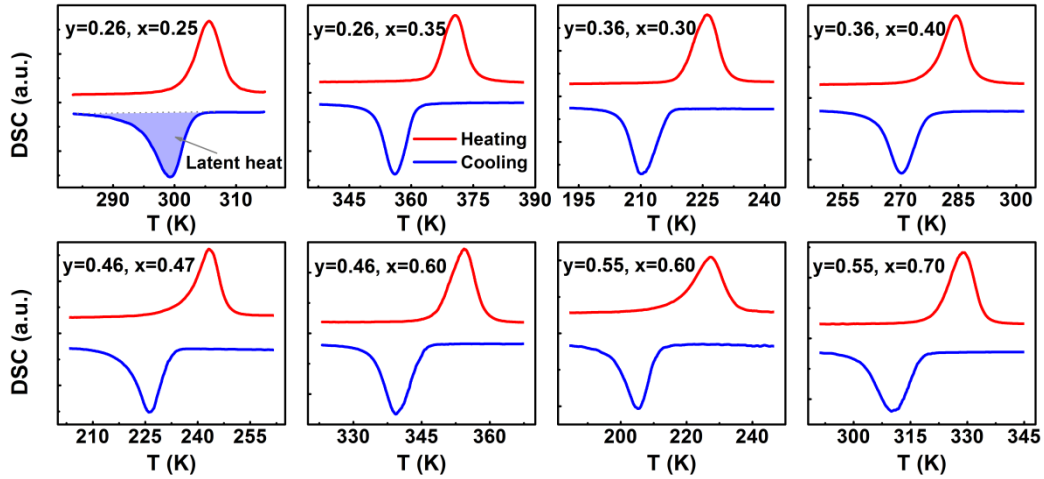

Figure S6. Low-temperature DSC analysis for selected samples of $Mn_{1-y}Fe_yNiGe_{1-x}Si_x$ for (a) y = 0.26, (b) y = 0.36, (c) y = 0.46 and (d) y = 0.55.

Table S2. Parameters of $Mn_{1-y}Fe_yNiGe_{1-x}Si_x$. ΔM is magnetization change across the martensitic transitions, T_t is martensitic transition temperature, T_{cr}^{dn} and T_{cr}^{up} are lower and upper critical temperatures of CTWs, respectively.

	x	ΔM [emu g^{-1}]	T_t [K]	T_{cr}^{dn} [K]	T_{cr}^{up} [K]	CTW width [K]
y = 0.26	**0.00**	-	**74**	**74**		360
	0.05	58.1	113			
	0.15	66.4	218			
	0.25	62.2	299			
	0.35	61.2	358			
	0.40	43.2	396			
	0.45	-	**434**		**434**	
y = 0.36	**0.15**	-	**51**	**51**		397
	0.20	58.5	120			
	0.30	64.9	212			
	0.40	59.8	270			
	0.50	54.5	348			
	0.60	44.9	426			
	0.63*	-	**448***		**448***	
y = 0.46	**0.30**	-	**40**			405
	0.35	57.4	118			
	0.40	65.1	161			
	0.47	61.9	230			
	0.53	62.7	276			
	0.60	55.0	342			
	0.70	44.7	398			
	0.75	32.8	**445**			
	0.45	-	**38**	**38**		

	0.50	53.1	114			
	0.60	59.5	209			
***y* = 0.55**	0.70	55.4	310			386
	0.80	43.3	397			
	0.82*	-	**424***		**424***	

*Extrapolated data.

Table S3. Calculated magnetic moments of $Mn_{0.5}Fe_{0.5}NiGe_{0.5}Si_{0.5}$.*

M_{total} [μ_B]	M_{Mn} [μ_B]	M_{Fe} [μ_B]	M_{Ni} [μ_B]	M_{Ge} [μ_B]	M_{Si} [μ_B]
2.36	2.74	1.74	0.12	-0.02	-0.02
	2.76	1.76	0.14		
			0.12		
			0.12		

*The energy favored atom configuration was chosen here. μ_B is Bohr magneton.

Table S4. Latent heats (ΔE), corresponding magnetostructural transition temperatures (T_t) and estimated total entropy changes (ΔS) of several representative compositions of $Mn_{1-y}Fe_yNiGe_{1-x}Si_x$ deprived from DSC data shown Figure S5 and S6.

	x	**ΔE [J g^{-1}]**	**T_t [K]**	**ΔS=ΔE/T_t [J Kg^{-1} K^{-1}]**
	0.15	10.8	218	49.54
	0.25	16.2	299	54.18
	0.35	18.3	358	51.12
***y* = 0.26**	0.60	16.4	561	29.23
	0.70	18.5	632	29.27
	0.85	18.1	861	21.02
	1.00	14.9	995	14.97
	0.30	12.9	212	60.85
	0.40	15.6	270	57.78
	0.60	26.6	426	62.44
***y* = 0.36**	0.65	20.7	466	44.42
	0.70	20.3	494	41.09
	0.85	23.2	632	36.71
	1.00	19.3	866	22.29
	0.47	13.3	230	57.83
	0.60	19.0	342	55.56
***y* = 0.46**	0.75	21.3	444	47.97
	0.80	21.8	488	44.67
	0.90	23.2	570	40.70
	1.00	29.7	648	45.83
	0.60	10.2	209	48.80
	0.70	19.7	310	63.55
***y* = 0.55**	0.84	21.9	443	49.44
	0.90	22.1	487	45.38
	1.00	22.7	554	40.98

Table S5. Absolute value of maximum entropy changes (|ΔS|) versus peak temperature for different magnetocaloric materials at field change ΔH = 20 kOe and ΔH = 50 kOe.

$La(Fe,Si)_{13}$ based	**T [K]**	**|ΔS| [J Kg^{-1} K^{-1}] (ΔH=20 kOe)**	**T [K]**	**|ΔS| [J Kg^{-1} K^{-1}] (ΔH=50 kOe)**	**Ref**
$LaFe_{11.4}Si_{1.6}$	208	14.3	208	19.4	[1]
$LaFe_{11.83}Si_{1.17}$	175	21.2	175	27.8	[2]
$LaFe_{11.7}Si_{1.3}$	183	22.9	183	26.0	[2]
$LaFe_{11.6}Si_{1.4}$	188	22.9	188	26	[2]
$LaFe_{11.5}Si_{1.5}$	194	20.8	194	24.8	[2]
$LaFe_{11.4}Si_{1.6}$	199	14.2	199	18.7	[2]
$LaFe_{11.3}Si_{1.7}$	206	11.9	206	17.6	[2]
$LaFe_{11.2}Si_{1.8}$	210	7.5	210	13	[2]
$LaFe_{11.0}Si_{2.0}$	221	4	221	7.9	[2]
$La_{0.9}Pr_{0.1}Fe_{11.5}Si_{1.5}$	191	24	191	26.1	[3]
$La_{0.7}Pr_{0.3}Fe_{11.5}Si_{1.5}$	185	28	185	30.5	[3]
$La_{0.5}Pr_{0.5}Fe_{11.5}Si_{1.5}$	181	30	181	32.4	[3]
$La_{0.9}Nd_{0.1}Fe_{11.5}Si_{1.5}$	192	23	192	25.9	[3]
$La_{0.7}Nd_{0.3}Fe_{11.5}Si_{1.5}$	188	29	188	32	[3]
$La_{0.7}Ce_{0.3}Fe_{11.5}Si_{1.5}$			173	23.8	[3]
$La_{0.7}Pr_{0.3}Fe_{11.2}Si_{1.8}$	204	14.4	204	19.4	[4]
$La_{0.7}Pr_{0.3}Fe_{11.0}Si_{2.0}$	218	6.2	218	11.4	[4]
$La_{0.7}Pr_{0.3}Fe_{11.4}Si_{1.6}$	198	12	204	17	[5]
$La_{0.7}Pr_{0.3}Fe_{11.34}Cu_{0.06}Si_{1.6}$			210	12	[5]
$La_{0.7}Pr_{0.3}Fe_{11.06}Cu_{0.34}Si_{1.6}$			230	5	[5]
$La_{0.8}Gd_{0.2}Fe_{11.4}Si_{1.6}$			200	14.8	[6]
$LaFe_{10.7}Co_{0.8}Si_{1.5}$	285	7	285	13.5	[7]
$La_{0.8}Pr_{0.2}Fe_{10.7}Co_{0.8}Si_{1.5}$	280	7.2	280	13.6	[7]
$La_{0.6}Pr_{0.4}Fe_{10.7}Co_{0.8}Si_{1.5}$	274	7.4	274	14.2	[7]
$La_{0.8}Pr_{0.5}Fe_{10.5}Co_{0.8}Si_{1.5}$	272	8.1	272	14.6	[7]
$La(Fe_{0.96}Co_{0.04})_{1.9}Si_{1.1}$	243	16.4	243	23	[8]
$La(Fe_{0.94}Co_{0.06})_{1.9}Si_{1.1}$	274	12.2	274	19.7	[8]
$La(Fe_{0.92}Co_{0.08})_{1.9}Si_{1.1}$	301	8.7	301	15.6	[8]
$LaFe_{11.2}Co_{0.7}Si_{1.1}$			274	20.3	[9]
$LaFe_{10.98}Co_{0.22}Si_{1.8}$	242	6.3	242	11.5	[10]
$LaFe_{11.12}Co_{0.71}Al_{1.17}$	279	4.6	279	9.1	[10]
$La(Fe_{0.98}Co_{0.02})_{11.7}Al_{1.3}$	198	5.9	198	10.6	[10]
$LaFe_{11.5}Si_{1.5}H_{0.3}$			224	17.4	[11]
$LaFe_{11.5}Si_{1.5}H_{0.9}$			272	16.9	[11]
$LaFe_{11.5}Si_{1.5}H_{1.3}$			288	17.0	[11]
$LaFe_{11.5}Si_{1.5}H_{1.8}$			341	20.5	[11]
$La(Fe_{0.99}Mn_{0.01})_{11.7}Si_{1.3}H_{\delta}$	336	16	336	23.4	[12]
$La(Fe_{0.98}Mn_{0.02})_{11.7}Si_{1.3}H_{\delta}$	312	13.0	312	17.7	[12]
$La(Fe_{0.97}Mn_{0.03})_{11.7}Si_{1.3}H_{\delta}$	287	11.0	287	15.9	[12]
$LaFe_{11.5}Si_{1.5}C_{0.2}$	225	18	225	22.8	[13]

$LaFe_{11.5}Si_{1.5}C_{0.5}$	241	7.4	241	12.7	[13]
$La_{0.8}Gd_{0.2}Fe_{11.4}Si_{1.6}B_{0.03}$			204	16	[6]
$La_{0.8}Gd_{0.2}Fe_{11.4}Si_{1.6}B_{0.06}$			205	15	[6]
$La_{0.8}Gd_{0.2}Fe_{11.4}Si_{1.6}B_{0.3}$			222	6.6	[6]
Gd			295	10.5	[14]
$Gd_5(Si,Ge)_4$	**T [K[**	**|ΔS| [J Kg^{-1} K^{-1}[(ΔH=20 kOe)**	**T [K]**	**|ΔS| [J Kg^{-1} K^{-1}[(ΔH=50 kOe)**	**Ref**
$Gd_5Si_2Ge_2$	276	14	276	18	[15]
$Gd_5Si_{1.8}Ge_{2.2}$	243	13	243	20	[16]
Gd_5Si_4	346	4.2	346	8.2	[17]
Gd_5Si_4			336	8.2*	[18]
$Gd_5Si_{3.5}Ge_{0.5}$			331	7.3*	[18]
Gd_5Si_3Ge			323	8.7*	[18]
$Gd_5Si_{2.5}Ge_{1.5}$			313	9.4*	[18]
$Gd_5Si_{2.06}Ge_{1.94}$			306	9.4*	[18]
$Gd_5Si_2Ge_2$			276	19*	[18]
$Gd_5Si_{1.72}Ge_{2.28}$			246	40*	[18]
$Gd_5Si_1Ge_3$			140	72*	[18]
$Gd_5Si_{0.9}Ge_{3.1}$			130	32*	[18]
$Gd_5Si_{0.8}Ge_{3.2}$			121	22*	[18]
$Gd_5Si_{0.33}Ge_{3.67}$			68	38*	[18]
$Gd_5Si_{0.15}Ge_{3.85}$			40	24*	[18]
$Gd_5(Ge_{0.9175}Si_{0.0825})_4$			76	61	[19]
$Gd_5(Ge_{0.75}Si_{0.25})_4$			143	69	[19]
$Gd_5(Ge_{0.57}Si_{0.43})_4$			244	40	[19]
$Gd_5(Ge_{0.\ 5}Si_{0.5})_4$			277	19	[19]
$Gd_5Si_{2.05}Ge_{1.95}$			279	9.2	[20]
Gd_5Ge_4			20	17	[18]
Gd_5Ge_4			40	26	[19]
$Gd_{2.5}Tb_{2.5}Si_4$	280	4	280	8	[17]
$Gd_3Tb_2Si_4$	296	4.1	296	8.	[17]
$Gd_{3.5}Tb_{1.5}Si_4$	311	4.5	311	9.5	[17]
$Gd_4Tb_1Si_4$	318	4	318	8.2	[17]
$Gd_{4.5}Tb_{0.5}Si_4$	334	4.1	334	8.2	[17]
$Gd_4Tb_1Si_4$	291	3	291	6.1	[17]
$Gd_{4.25}Tb_{0.75}Si_4$	304	3.6	304	7.5	[17]
$Gd_{4.5}Tb_{0.5}Si_4$	316	4	316	8	[17]
$Gd_5Ge_{1.9}Si_2Fe_{0.1}$			300	8	[21]
$Gd_5Si_{2.02}Ge_{1.92}Mn_{0.06}$			275	11.6	[20]
$Gd_5Si_{1.97}Ge_{1.87}Mn_{0.16}$			294	7	[20]
$Gd_5Si_{1.985}Ge_{1.985}Ga_{0.03}$			276	8.4	[22]
$Gd_5Si_{1.975}Ge_{1.975}Ga_{0.05}$			297	6.5	[22]
$Gd_5Si_{1.935}Ge_{1.935}Ga_{0.13}$			297	6.1	[22]

$RE_5(Si,Ge)_4$	T [K]	$\|\Delta S\|$ [J Kg^{-1} K^{-1}] (ΔH=20 kOe)	T [K]	$\|\Delta S\|$ [J Kg^{-1} K^{-1}] (ΔH=50 kOe)	Ref
$Tb_5Si_2Ge_2$	102	10	102	22	[23]
Tb_5Si_4	225	5	225	10	[23]
Tb_5Ge_4	90	1	90	4	[23]
$Tb_5Si_2Ge_2$			102	13	[24]
Dy_5Si_4			141	12.8	[25]
$Dy_5(Si_{3.5}Ge_{0.5})$			136	11.9	[25]
$Dy_5(Si_3Ge)$			65	33.2	[25]
$Dy_5(Si_{2.3}Ge_{1.5})$			56	7.0	[25]
$Dy_5(Si_2Ge_2)$			54	7.0	[25]
$Dy_5(SiGe_3)$			50	7.0	[25]
Dy_5Ge_4			46	7	[25]
$Ho_5Si_2Ge_2$			25	58.5	[26]
Tb_5Si_4	223	4.5	223	9	[17]
Hex RE compounds	**T [K]**	**$\|\Delta S\|$ [J Kg^{-1} K^{-1}] (ΔH=20 kOe)**	**T [K]**	**$\|\Delta S\|$ [J Kg^{-1} K^{-1}] (ΔH=50 kOe)**	**Ref**
GdRhSn	16	4	16	6.5	[27]
HoPdAl (hexagonal)	10	3	10	13.7	[28]
HoPdAl (orthorhombic)	12	11.4	12	22.8	[28]
TbPdAl	43	5.9	43	11.4	[29]
HoCuSi	8	16	8	34	[30]
HoNiCuIn	10	12.5	10	20.2	[31]
Er_2In	46	7.9	46	16	[32]
Tb_2In	165	3.5	165	6.6	[33]
Dy_2In	130	4.6	130	9.2	[34]
Ho_2In	85	5.0	85	11.2	[35]
GdCoAl	100	4.9	100	10.4	[36]
TbCoAl	70	5.3	70	10.5	[36]
DyCoAl	37	9.2	37	16.3	[36]
HoCoAl	10	12.5	10	21.5	[36]
$(Gd_{0.5}Dy_{0.25}Er_{0.25})CoAl$	45	6.3	45	14	[36]
$RECo_2$	**T [K]**	**$\|\Delta S\|$ [J Kg^{-1} K^{-1}] (ΔH=20 kOe)**	**T [K]**	**$\|\Delta S\|$ [J Kg^{-1} K^{-1}] (ΔH=50 kOe)**	**Ref**
$GdCo_{0.7}Mn_{1.3}$			300	3.35	[37]
$GdCo_{0.6}Mn_{1.4}$			270	3.82	[37]
$GdCo_{0.4}Mn_{1.6}$			210	3.86	[37]
$GdCo_{0.2}Mn_{1.8}$			140	4.11	[37]
$HoCo_2$			75	22.5	[38]
$DyCo_2$			140	11	[38]
$TbCo_2$			227	6.5	[38]
$ErCo_2$			33.6	38	[39]
$Er(Co_{0.95}Si_{0.05})_2$			60	22	[39]
$Er(Co_{0.85}Si_{0.15})_2$			63	8	[39]

$Er(Co_{0.975}Si_{0.025})_2$			48	32	[38]
$Dy_{0.7}Y_{0.3}Co_2$			115	15	[38]
$Dy_{0.9}Y_{0.1}Co_2$			130	14	[38]
$Ho(Co_{0.95}Si_{0.05})_2$			100	20	[38]
$Ho(Co_{0.975}Si_{0.025})_2$			80	23	[38]
$ErCo_2$			38	23	[40]
$Er(Co_{0.95}Fe_{0.05})_2$			70	13	[40]
$Er(Co_{0.9}Fe_{0.1})_2$			150	6.5	[40]
$ErCo_{1.8}Mn_{0.2}$			86	6.97	[41]
$HoCo_{1.8}Mn_{0.2}$			156	5.36	[41]
$DyCo_{1.8}Mn_{0.2}$			220	4.57	[41]
$TbCo_{1.8}Mn_{0.2}$			312	3.2	[41]
$MnFeX$ (Fe_2P type)	**T [K]**	**$\|\Delta S\|$ [J Kg^{-1} K^{-1}] (ΔH=20 kOe)**	**T [K]**	**$\|\Delta S\|$ [J Kg^{-1} K^{-1}] (ΔH=50 kOe)**	**Ref**
$MnFeP_{0.45}As_{0.55}$	305	14.5	309	18	[42]
$MnFeP_{0.5}As_{0.5}$	288	16	288	21	[43]
$Mn_{1.1}Fe_{0.9}P_{0.5}As_{0.5}$	280	26	280	28	[43]
$Mn_{1.3}Fe_{0.7}P_{0.6}Si_{0.2}Ge_{0.15}$	246	2.5	246	5.7	[44]
$Mn_{1.2}Fe_{0.8}P_{0.6}Si_{0.2}Ge_{0.15}$	285	5.3	285	11	[44]
$Mn_{1.1}Fe_{0.9}P_{0.6}Si_{0.2}Ge_{0.15}$	325	12	325	16	[44]
Mn $FeP_{0.6}Si_{0.2}Ge_{0.15}$	333	11	333	17.5	[44]
$Mn_{1.2}Fe_{0.75}P_{0.5}Si_{0.5}$			304	31	[45]
$Mn_{1.25}Fe_{0.70}P_{0.5}Si_{0.5}$			285	27	[45]
$Mn_{1.3}Fe_{0.65}P_{0.5}Si_{0.5}$			269	21	[45]
$Mn_{1.25}Fe_{0.7}P_{0.55}Si_{0.45}$			246	33	[45]
$Mn_{1.25}Fe_{0.7}P_{0.45}Si_{0.55}$			323	19	[45]
$Mn_{1.2}Fe_{0.8}P_{0.75}Ge_{0.25}$	288	20.3	288	25	[46]
MnAs	**T [K]**	**$\|\Delta S\|$ [J Kg^{-1} K^{-1}] (ΔH=20 kOe)**	**T [K]**	**$\|\Delta S\|$ [J Kg^{-1} K^{-1}] (ΔH=50 kOe)**	**Ref**
MnAs	315	38	315	41	[47]
MnAs			317	41	[48]
$MnAs_{0.95}Sb_{0.05}$			308	32	[48]
$MnAs_{0.85}Sb_{0.15}$			260	30	[48]
$MnAs_{0.70}Sb_{0.30}$	225	23	225	27	[48]
$MnAs_{0.6}Sb_{0.4}$	214	7	214	14	[48]
$MnAs_{0.95}Sb_{0.05}$	310	27	310	33	[47]
$MnAs_{0.9}Sb_{0.1}$	285	25	285	32	[47]
$Mn_{0.994}Cr_{0.006}As$			292	13.7	[49]
$Mn_{0.99}Cr_{0.01}As$			267	20.2	[49]
$MM'X$ (Ni_2In type)	**T [K]**	**$\|\Delta S\|$ [J Kg^{-1} K^{-1}] (ΔH=20 kOe)**	**T [K]**	**$\|\Delta S\|$ [J Kg^{-1} K^{-1}] (ΔH=50 kOe)**	**Ref**
$MnNi_{0.77}Fe_{0.23}Ge$	265	7	265	19	[50]
$Mn_{0.82}Fe_{0.18}NiGe$	203	13	203	31	[50]
$Mn_{0.93}Cr_{0.03}CoGe$			300	22	[51]

$Mn_{0.94}Ti_{0.06}CoGe$			232	11.3	[52]
$MnCoGe_{0.99}Al_{0.01}$			357	29.2	[53]
$MnCoGe_{0.98}Al_{0.02}$			323	35.9	[53]
$MnCoGe_{0.97}Al_{0.03}$			180	5.7	[53]
$Mn_{0.9}Co_{0.1}NiGe$			236	40	[54]
$Mn_{0.965}CoGe$	289	10	289	26	[55]
$Mn_{1.05}Ni_{0.85}Ge$	135	14	135	27	[56]
$Mn_{1.045}Ni_{0.855}Ge$	160	12	160	25	[56]
$(MnNiSi)_{0.56}(FeNiGe)_{0.44}$			187	11.5	[57]
$(MnNiSi)_{0.54}(FeNiGe)_{0.46}$			192	10.8	[57]
$(MnNiSi)_{0.52}(FeNiGe)_{0.48}$			174	8.4	[57]
$Mn_{0.89}Cr_{0.11}NiGe$	275	11	275	28	[58]
$Mn_{0.92}Cu_{0.08}CoGe$	321	21	321	53.3	[59]
$Mn_{0.91}Cu_{0.09}CoGe$	289	16	289	41.2	[59]
$Mn_{0.9}Cu_{0.1}CoGe$	249	15	249	36.4	[59]
$MnCoGeB_{0.02}$	287	21	287	47.3	[60]
$MnCoGeB_{0.03}$	275	16	275	37.7	[60]
$MnCoGeB_{0.05}$			260	3.4	[60]
Heusler alloys	**T [K]**	**$\|\Delta S\|$ [J Kg^{-1} K^{-1}] (ΔH=20 kOe)**	**T [K]**	**$\|\Delta S\|$ [J Kg^{-1} K^{-1}] (ΔH=50 kOe)**	**Ref**
$Ni_{50}Mn_{37}Sn_{13}$			189	18	[61]
$Ni_{50}Mn_{35}Sn15$			307	15	[61]
$Ni_{52.6}Mn_{23.1}Ga_{24.3}$	304	6.5	304	18	[62]
$Ni_2Mn_{0.755}Cu_{0.245}Ga$	298	29	298	45	[63]
$Ni_2Mn_{0.75}Cu_{0.25}Ga$	308	29	308	65	[63]
$Ni_2Mn_{0.74}Cu_{0.26}Ga$	302	25	302	43	[63]
$Ni_{50}Mn_{34}In_{16}$	243	3	243	8	[64]
$Ni_{50}Mn_{34}In_{14}Ga_2$	275	3	275	9	[64]
$Ni_2Mn_{1.2}Ga_{0.8}$			352	7.3	[65]
$Ni_{1.9}Mn_{1.3}Ga_{0.8}$			365	9.6	[65]
$Ni_{43}Mn_{43}Co_3Sn_{11}$	188	18	188	33	[66]
$Ni_{50}Mn_{37}Sn_{13}$			280	0.2	[67]
$Ni_{49}M_{n38}Sn_{13}$			270	2.2	[67]
$Ni_{48}Mn_{39}Sn_{13}$			226	12	[67]
$Ni_{47}Mn_{40}Sn_{13}$			187	34	[67]
$Ni_{46}Mn_{41}Sn_{13}$			132	11	[67]
$Ni_{43}Mn_{46}Sn_{11}$			205	10.4	[68]
$Ni_{43}Mn_{46}Sn_{10.5}Al_{0.5}$			236	8.1	[68]
$Ni_{43}Mn_{46}Sn_{10}Al_1$			264	3.9	[68]
$Ni_{43}Mn_{46}Sn_9Al_2$			297	1.4	[68]
$Ni_{51}Mn_{32.8}In_{16.2}$			253	19.2	[69]
$Ni_{51}Mn_{32.8}In_{16.2}H_{1.4}$			245	17.5	[69]
$Ni_{44.4}Mn_{44.1}Sn_{11.5}$	260	10.6			[70]
$Ni_{44.2}Mn_{39.3}Fe_{4.9}Sn_{11.6}$	284	6.4			[70]

$Ni_{44.5}Mn_{37}Fe_{6.7}Sn_{11.8}$	293	5.6			[70]
$Ni_{49}Co_1Mn_{37}Sn_{13}$	290	3	290	9	[71]
$Ni_{47}Co_3Mn_{37}Sn_{13}$	255	3	255	9	[71]
$Ni_{49}Fe_1Mn_{37}Sn_{13}$	240	6	240	16	[71]
$Ni_{47}Fe_3Mn_{37}Sn_{13}$	175	11	175	30	[71]
$Ni_{55.4}Mn_{20}Ga_{24.6}$	313	40	313	85	[72]
$Ni_{51}Mn_{32.4}In_{16.6}$	246	16	246	17.2	[69]
$Ni_{51}Mn_{32.4}In_{16.6}H_{5.2}$	219	9	219	13	[69]
$Ni_{43}Mn_{42}Co_4Sn_{11}$			220	19	[73]
$Ni_{42}Co_8Mn_{30}Fe_2Ga_{18}$	205	11	205	31	[74]
$Ni_{46}Co_4Mn_{38}Sb_{12}$			295	32.3	[75]
$Ni_{52}Mn_{26}Ga_{22}$	355	16	355	30	[76]
Present work	**T [K]**	**$\|\Delta S\|$ [J Kg^{-1} K^{-1}] (ΔH=20 kOe)**	**T [K]**	**$\|\Delta S\|$ [J Kg^{-1} K^{-1}] (ΔH=50 kOe)**	
$Mn_{0.64}Fe_{0.36}NiGe_{0.8}Si_{0.2}$	127	10.7	127	27.9	
$Mn_{0.64}Fe_{0.36}NiGe_{0.7}Si_{0.3}$	219	11.4	219	33.6	
$Mn_{0.64}Fe_{0.36}NiGe_{0.6}Si_{0.4}$	277	11.6	277	30.5	
$Mn_{0.64}Fe_{0.36}NiGe_{0.5}Si_{0.5}$	353	9.6	353	24.7	
$Mn_{0.64}Fe_{0.36}NiGe_{0.4}Si_{0.6}$	437	7.6	437	27.4	

*the data calculated from the entropy change per unit volume with assuming density of 7.5 g cm^{-3}

References

[1] F.-X. Hu, B.-G. Shen, J.-R. Sun, Z.-H. Cheng, G.-H. Rao, X.-X. Zhang, *Appl. Phys. Lett.* **2001**, *78*, 3675.

[2] B. G. Shen, J. R. Sun, F. X. Hu, H. W. Zhang, Z. H. Cheng, *Adv. Mater.* **2009**, *21*, 4545.

[3] S. Jun, L. Yang-Xian, S. Ji-Rong, S. Bao-Gen, *Chin. Phys. B* **2009**, *18*, 2058.

[4] J. Shen, Y.-X. Li, Q.-Y. Dong, J.-R. Sun, *J. Magn. Magn. Mater.* **2009**, *321*, 2336.

[5] M. F. Md Din, J. L. Wang, R. Zeng, P. Shamba, J. C. Debnath, S. X. Dou, *Intermetallics* **2013**, *36*, 1.

[6] P. Shamba, R. Zeng, J. L. Wang, S. J. Campbell, S. X. Dou, *J. Magn. Magn. Mater.* **2013**, *331*, 102.

[7] J. Shen, B. Gao, Q.-Y. Dong, Y.-X. Li, F.-X. Hu, J.-R. Sun, B.-G. Shen, *J. Phys. D - Appl. Phys.* **2008**, *41*, 245005.

[8] F. X. Hu, J. Gao, X. L. Qian, M. Ilyn, A. M. Tishin, J. R. Sun, B. G. Shen, *J. Appl. Phys.* **2005**, *97*, 10M303.

[9] F.-X. Hu, B.-g. Shen, J.-r. Sun, G.-j. Wang, Z.-h. Cheng, *Appl. Phys. Lett.* **2002**, *80*, 826.

[10] F.-X. Hu, S. B.-g. Shen, J.-r. Sun, X.-X. Zhang, *Chin. Phys.* **2000**, *9*, 550.

[11] Y. F. Chen, F. Wang, B. G. Shen, F. X. Hu, J. R. Sun, G. J. Wang, Z. H. Cheng, *J. Phys. - Condens. Matter* **2003**, *15*, L161.

[12] W. Fang, C. Yuan-Fu, W. Guang-Jun, S. Ji-Rong, S. Bao-Gen, *Chin. Phys.* **2003**, *12*, 911.

[13] Y.-f. Chen, F. Wang, B.-G. Shen, J.-R. Sun, G.-J. Wang, F.-X. Hu, Z.-H. Cheng, T. Zhu, *J. Appl. Phys.* **2003**, *93*, 6981.

[14] V. K. Pecharsky, K. A. Gschneidner Jr, *J. Magn. Magn. Mater.* **1999**, *200*, 44.

[15] V. K. Pecharsky, J. K. A. Gschneidner, *Phys. Rev. Lett.* **1997**, *78*, 4494.

[16] F. Casanova, X. Batlle, A. Labarta, J. Marcos, L. Mañosa, A. Planes, *Phys. Rev. B* **2002**, *66*, 100401.

[17] Y. I. Spichkin, V. K. Pecharsky, K. A. Gschneidner, *J. Appl. Phys.* **2001**, *89*, 1738.

[18] K. A. Gschneidner, V. K. Pecharsky, *Annu. Rev. Mater. Sci.* **2000**, *30*, 387.

[19] V. K. Pecharsky, K. A. Gschneidner, *Appl. Phys. Lett.* **1997**, *70*, 3299.

[20] E. Yüzüak, I. Dincer, Y. Elerman, *J. Rare Earths* **2010**, *28*, 477.

[21] V. Provenzano, A. J. Shapiro, R. D. Shull, *Nature* **2004**, *429*, 853.

[22] S. Aksoy, A. Yucel, Y. Elerman, T. Krenke, M. Acet, X. Moya, L. Mañosa, *J. Alloys Compd.* **2008**, *460*, 94.

[23] L. Morellon, C. Magen, P. A. Algarabel, M. R. Ibarra, C. Ritter, *Appl. Phys. Lett.* **2001**, *79*, 1318.

[24] L. Morellon, Z. Arnold, C. Magen, C. Ritter, O. Prokhnenko, Y. Skorokhod, P. A. Algarabel, M. R. Ibarra, J. Kamarad, *Phys. Rev. Lett.* **2004**, *93*, 137201.

[25] V. V. Ivtchenko, V. K. Pecharsky, K. A. J. Gschneidner, in *Advanced Cryogenic Engineering*, Vol. 46, 2000, 405.

[26] N. P. Thuy, Y. Y. Chen, Y. D. Yao, C. R. Wang, S. H. Lin, J. C. Ho, T. P. Nguyen, P. D. Thang, J. C. P. Klaasse, N. T. Hien, L. T. Tai, *J. Magn. Magn. Mater.* **2003**, *262*, 432.

[27] S. Gupta, K. G. Suresh, A. K. Nigam, Y. Mudryk, D. Paudyal, V. K. Pecharsky, K. A. Gschneidner, *J. Alloys Compd.* **2014**, *613*, 280.

[28] Z. Xu, B. Shen, *Sci. China - Technol. Sci.* **2011**, *55*, 445.

[29] J. Shen, Z.-Y. Xu, H. Zhang, X.-Q. Zheng, J.-F. Wu, F.-X. Hu, J.-R. Sun, B.-g. Shen, *J. Magn. Magn. Mater.* **2011**, *323*, 2949.

[30] J. Chen, B. G. Shen, Q. Y. Dong, F. X. Hu, J. R. Sun, *Appl. Phys. Lett.* **2010**, *96*, 152501.

[31] Z.-J. Mo, J. Shen, L.-Q. Yan, C.-C. Tang, X.-N. He, X. Zheng, J.-F. Wu, J.-R. Sun, B.-G. Shen, *J. Magn. Magn. Mater.* **2014**, *354*, 49.

[32] H. Zhang, B. G. Shen, Z. Y. Xu, J. Chen, J. Shen, F. X. Hu, J. R. Sun, *J. Alloys Compd.* **2011**, *509*, 2602.

[33] Q. Zhang, J. H. Cho, J. Du, F. Yang, X. G. Liu, W. J. Feng, Y. J. Zhang, J. Li, Z. D. Zhang, *Solid State Commun.* **2009**, *149*, 396.

[34] Q. Zhang, X. G. Liu, F. Yang, W. J. Feng, X. G. Zhao, D. J. Kang, Z. D. Zhang, *J. Phys. D - Appl. Phys.* **2009**, *42*,

055011.

[35] Q. Zhang, J. H. Cho, B. Li, W. J. Hu, Z. D. Zhang, *Appl. Phys. Lett.* **2009**, *94*, 182501.

[36] X. X. Zhang, F. W. Wang, G. H. Wen, *J. Phys. - Condens. Matter* **2001**, *13*, L747.

[37] J. Y. Zhang, J. Luo, J. B. Li, J. K. Liang, Y. C. Wang, L. N. Ji, Y. H. Liu, G. H. Rao, *Solid State Commun.* **2007**, *143*, 541.

[38] N. H. Duc, D. T. Kim Anh, P. E. Brommer, *Phys. B* **2002**, *319*, 1.

[39] N. H. Duc, P.E. Brommer, K. H. J. Buschow, *Handbook on Magnetic Materials*, Vol. 17, 1999, Ch. 5.

[40] X. B. Liu, Z. Altounian, *J. of Appl. Phys.* **2008**, *103*, 07B304.

[41] A. K. Pathak, I. Dubenko, S. Stadler, N. Ali, *J. Magn. Magn. Mater.* **2011**, *323*, 2436.

[42] O. Tegus, E. Bruck, K. H. J. Buschow, F. R. de Boer, *Nature* **2002**, *415*, 150.

[43] E. Brück, O. Tegus, X. W. Li, F. R. de Boer, K. H. J. Buschow, *Phys. B* **2003**, *327*, 431.

[44] G. F. Wang, Z. R. Zhao, L. Song, O. Tegus, *J. Alloys Compd.* **2013**, *554*, 208.

[45] N. H. Dung, L. Zhang, Z. Q. Ou, E. Brück, *Scr. Mater.* **2012**, *67*, 975.

[46] N. T. Trung, J. C. P. Klaasse, O. Tegus, D. T. Cam Thanh, K. H. J. Buschow, E. Brück, *J. Phys. D - Appl. Phys.* **2010**, *43*, 015002.

[47] H. Wada, Y. Tanabe, *Appl. Phys. Lett.* **2001**, *79*, 3302.

[48] H. Wada, K. Taniguchi, Y. Tanabe, *Mater. Trans.* **2002**, *43*, 73.

[49] N. K. Sun, W. B. Cui, D. Li, D. Y. Geng, F. Yang, Z. D. Zhang, *Appl. Phys. Lett.* **2008**, *92*, 072504.

[50] E. Liu, W. Wang, L. Feng, W. Zhu, G. Li, J. Chen, H. Zhang, G. Wu, C. Jiang, H. Xu, F. de Boer, *Nat. Commun.* **2012**, *3*, 873.

[51] L. Caron, N. T. Trung, E. Brück, *Phys. Rev. B* **2011**, *84*, 020414.

[52] P. Shamba, J. L. Wang, J. C. Debnath, S. J. Kennedy, R. Zeng, M. F. Din, F. Hong, Z. X. Cheng, A. J. Studer, S. X. Dou, *J. Phys. - Condens. Matter* **2013**, *25*, 056001.

[53] L. F. Bao, F. X. Hu, R. R. Wu, J. Wang, L. Chen, J. R. Sun, B. G. Shen, L. Li, B. Zhang, X. X. Zhang, *J. Phys. D - Appl. Phys.* **2014**, *47*, 055003.

[54] E. K. Liu, H. G. Zhang, G. Z. Xu, X. M. Zhang, R. S. Ma, W. H. Wang, J. L. Chen, H. W. Zhang, G. H. Wu, L. Feng, X. X. Zhang, *Appl. Phys. Lett.* **2013**, *102*, 122405.

[55] E. K. Liu, W. Zhu, L. Feng, J. L. Chen, W. H. Wang, G. H. Wu, H. Y. Liu, F. B. Meng, H. Z. Luo, Y. X. Li, *Europhys. Lett.* **2010**, *91*, 17003.

[56] C. L. Zhang, D. H. Wang, Q. Q. Cao, Z. D. Han, H. C. Xuan, Y. W. Du, *Appl. Phys. Lett.* **2008**, *93*, 122505.

[57] C. L. Zhang, D. H. Wang, Z. D. Han, B. Qian, H. F. Shi, C. Zhu, J. Chen, T. Z. Wang, *Appl. Phys. Lett.* **2013**, *103*, 132411.

[58] A. P. Sivachenko, V. I. Mityuk, V. I. Kamenev, A. V. Golovchan, V. I. Val'kov, I. F. Gribanov, *Low Temp. Phys.* **2013**, *39*, 1051.

[59] T. Samanta, I. Dubenko, A. Quetz, S. Stadler, N. Ali, *Appl. Phys. Lett.* **2012**, *101*, 242405.

[60] N. T. Trung, L. Zhang, L. Caron, K. H. J. Buschow, E. Brück, *Appl. Phys. Lett.* **2010**, *96*, 172504.

[61] T. Krenke, E. Duman, M. Acet, E. F. Wassermann, X. Moya, L. Manosa, A. Planes, *Nat. Mater.* **2005**, *4*, 450.

[62] F.-X. Hu, B.-G. Shen, J.-R. Sun, G.-H. Wu, *Phys. Rev. B* **2001**, *64*, 132412.

[63] S. Stadler, M. Khan, J. Mitchell, N. Ali, A. M. Gomes, I. Dubenko, A. Y. Takeuchi, A. P. Guimarães, *Appl. Phys. Lett.* **2006**, *88*, 192511.

[64] S. Aksoy, T. Krenke, M. Acet, E. F. Wassermann, X. Moya, L. s. Mañosa, A. Planes, *Appl. Phys. Lett.* **2007**, *91*, 241916.

[65] F. Albertini, A. Paoluzi, L. Pareti, M. Solzi, L. Righi, E. Villa, S. Besseghini, F. Passaretti, *J. Appl. Phys.* **2006**, *100*, 023908.

[66] B. Gao, F. X. Hu, J. Shen, J. Wang, J. R. Sun, B. G. Shen, *J. Magn. Magn. Mater.* **2009**, *321*, 2571.

[67] S. E. Muthu, N. V. R. Rao, M. M. Raja, D. M. R. Kumar, D. M. Radheep, S. Arumugam, *J. Phys. D - Appl. Phys.* **2010**, *43*, 425002.

[68] J. Chen, Z. Han, B. Qian, P. Zhang, D. Wang, Y. Du, *J. Magn. Magn. Mater.* **2011**, *323*, 248.

[69] F. X. Hu, J. Wang, L. Chen, J. L. Zhao, J. R. Sun, B. G. Shen, *Appl. Phys. Lett.* **2009**, *95*, 112503.

[70] J. L. Yan, Z. Z. Li, X. Chen, K. W. Zhou, S. X. Shen, H. B. Zhou, *J. Alloys Compd.* **2010**, *506*, 516.

[71] T. Krenke, E. P. Duman, M. Acet, X. Moya, L. S. Mañosa, A. Planes, *J. Appl. Phys.* **2007**, *102*, 033903.

[72] M. Pasquale, C. P. Sasso, L. H. Lewis, L. Giudici, T. Lograsso, D. Schlagel, *Phys. Rev. B* **2005**, *72*, 094435.

[73] N. M. Bruno, C. Yegin, I. Karaman, J.-H. Chen, J. H. Ross, J. Liu, J. Li, *Acta Mater.* **2014**, *74*, 66.

[74] A. K. Pathak, I. Dubenko, H. E. Karaca, S. Stadler, N. Ali, *Appl. Phys. Lett.* **2010**, *97*, 062505.

[75] A. K. Nayak, K. G. Suresh, A. K. Nigam, A. A. Coelho, S. Gama, *J. Appl. Phys.* **2009**, *106*, 053901.

[76] Z. Li, Y. Zhang, C. F. Sánchez-Valdés, J. L. Sánchez Llamazares, C. Esling, X. Zhao, L. Zuo, *Appl. Phys. Lett.* **2014**, *104*, 044101.